



Binder-free copper hexacyanoferrate electrode prepared by pulse galvanostatic electrochemical deposition for aqueous-based Al-ion batteries

Pourya Parvizi ^a, Mahdi Kazazi^{*a}

^a Department of Materials Engineering, Faculty of Engineering, Malayer University, P.O. Box 65719-95863, Malayer, Iran

P A P E R I N F O

Paper history:

Received 23 December 2018

Accepted in revised form 12 March 2019

Keywords:

Electrochemical deposition

Copper hexacyanoferrate

Al-ion batteries

Aqueous electrolyte

Cathode

A B S T R A C T

Copper hexacyanoferrate (CuHCF) nanoparticles with tunnel-like Prussian blue structure were deposited on a graphite substrate via pulse galvanostatic electrodeposition at 25 mA cm⁻² with two 0.1 s periods of on/off-time. The prepared electrode reversibly showed the intercalation/de-intercalation ability of Al ions in aqueous solution. The crystal structure of the as-prepared CuHCF film was characterized by X-ray diffraction (XRD) analysis. The surface morphology of the film was examined by a field-emission scanning electron microscope (FESEM). Moreover, the electrochemical energy storage performance of the prepared binder-free electrode was inspected by cyclic voltammetry (CV) and galvanostatic charge-discharge (GCD) measurements at various rates in aqueous-based aluminum sulfate electrolyte. The CuHCF was verified that can be a promising cathode material for the aqueous Al-ion batteries. The prepared CuHCF electrode exhibited a high specific capacity of 77.7 mAh g⁻¹ and a good rate capability with 67.1% capacitance retention rate at a current density of 50 mA g⁻¹ and 400 mA g⁻¹, respectively. Furthermore, after 400 cycles at 400 mA g⁻¹, the electrode showed a good cycle performance with a capacity retention rate of 74.4%.

1. INTRODUCTION

Running out of fossil fuels and their pollutions has resulted in using clean and renewable energy. Due to the rapid growth of various portable applications such as electric and hybrid electric vehicles (EVs and HEVs), it is necessary to develop rechargeable batteries having high energy density, high power density, and high safety. Lithium-ion batteries (LIBs) have been the mainstay of high energy storage devices because of a good electrochemical performance including high specific capacity and good cycle life [1-3]. However, there is an increase in demand for alternative energy storage devices which have high energy and power density and low cost without consist of safety and lifetime [4].

The Li-ion batteries have had significant challenges in increasing the amount of stored energy without affecting the overall lifetime and ability to deliver the stored energy. Unlike monovalent Li⁺ ions, multivalent rechargeable batteries offer a potential solution for aforementioned problems [5-8]. The aluminum-based rechargeable batteries are attractive alternatives than the

other ones, which are based on conventional chemistries, because of the high charge-storage capacity and relatively low cost of the aluminum. It should be mentioned that only one-third of Al³⁺ ions need to be intercalated and de-intercalated from an electrode in comparison with the Li⁺ ions due to the trivalent nature of these batteries. This reduces the probability of lattice distortion and undesirable structural changes [9].

Despite various research works carried out about the trivalent Al ion battery chemistry, few instances of electrode materials such as V₂O₅, VO₂ and TiO₂ have been proposed which have the capability of Al ion intercalation [8,10-12]. Recently, Kazazi et al. have shown that TiO₂/carbon nanotubes composite can enhance the conductivity of the electrode and Al ion diffusion which causes an increase in the capacity of the TiO₂ cathode material in the Al-ion battery [12]. Metal hexacyanometallates are a class of inorganic coordination polymers which are capable of storing and giving up electrons through the process of reduction and oxidation. These materials can be represented by a general formula of A_xSP(CN)₆, wherein S and P metal

^{*} Corresponding Author's Email: m_kazazi@malayer.ac.ir (M. Kazazi)

ions are coordinated to nitrogen and carbon end of the cyanide ligand (CN), respectively, and A represents the large interstitial tunnel sites that are populated by the hydrated cations in order to maintain charge neutrality of the host lattice [13-17]. In the research conducted by Liu et al. [18], it was well shown that Al ions can be reversibly inserted and extracted from the copper hexacyanoferrate (CuHCF) active material in an aqueous-based electrolyte.

In traditional preparation of energy storage electrodes, polyvinylidene fluoride (PVDF) binder is used to paste the active materials onto the surface of current collectors. The utilization of such an insulating binder reduces the conductivity and the electrode capacity. In contrast, the electrochemical deposition method along with synthesis can directly deposit the active material onto the current collector without the binder; therefore, it can greatly improve the charge storage performance of the electrode. Several successes established upon Al ion insertion into TiO₂ have motivated us to explore new cathode materials for the aqueous Al-ion batteries. However, the CuHCF active material was deposited by a simple pulse galvanostatic electrodeposition route on the surface of graphite substrate. Moreover, the energy storage performance of the as-prepared electrode as the cathode of aqueous-based Al-ion batteries was studied by cyclic voltammetry (CV) and galvanostatic charge-discharge measurements. To the best of our knowledge, no metal hexacyanoferrate was deposited via the pulse galvanostatic electrodeposition thus far.

2. EXPERIMENTAL

2.1. MATERIALS

All the materials such as K₃[Fe(CN)₆], NaCl and CuNO₃.6(H₂O) were of analytical grade (Merck company) and used without further purification.

2.2. ELECTRODEPOSITION OF CUHCF

Before the deposition process, the graphite substrates (1cm × 1cm) were mechanically polished with SiC#1000 paper grit. After that, the graphite substrates were functionalized in a concentrated mixture of [H₂SO₄]/[HNO₃] (3:1) at 60°C for 6 h to improve its hydrophilicity which is followed by washing with the distilled water and ethanol and drying in an oven at 100°C. The employed electrolyte was an aqueous solution of 0.5 M NaCl, 0.3 mM CuNO₃.6(H₂O) and 0.3 mM K₃[Fe(CN)₆] for electrodeposition process. The CuHCF was deposited onto the graphite substrate at room temperature by applying a pulse constant current density of 25 mA cm⁻² with both on-time and off-time of 0.1 s for 30 min. Then, the as-prepared CuHCF electrode was washed with the double-distilled water and finally dried at room temperature.

2.3. FILM CHARACTERIZATION

The structural evaluation of the as-prepared CuHCF electrode was performed by X-ray diffraction (XRD) using a Philips diffractometer with Cu K α radiation at 2 θ ranging from 10° to 80°. The surface morphology of the CuHCF was studied by a field-emission scanning electron microscope (FESEM, MIRA3 TESCAN).

2.4. ELECTROCHEMICAL MEASUREMENTS

The electrochemical performance of the as-prepared CuHCF as cathode material of the Al-ion batteries was investigated by cyclic voltammetry (CV) and galvanostatic charge-discharge measurements (GCD) in a conventional three-electrode cell. The CuHCF, silver/silver chloride and graphite electrode were used as a working, reference and counter electrode, correspondingly. Furthermore, 0.5 M Al₂(SO₄)₃ aqueous solution was implemented as the electrolyte. CV and GCD measurements were conducted using an Ivium electrochemical workstation. In detail, the CV was carried out at a scan rate of 5 and 10 mV s⁻¹ between 0.2 to 1.2 V (vs. Ag/AgCl). The typical charge and discharge curves were also obtained at various current densities of 50, 100, 200 and 400 mA g⁻¹ in the same potential range.

3. RESULTS AND DISCUSSION

3.1. ELECTRODE CHARACTERIZATION

Figure 1 shows the XRD pattern of the electrode. The as-prepared CuHCF electrode material shows a high crystallinity degree and all the reflections are indexed as the face-centered cubic Prussian blue structure (ICDD PDF card no. 01-086-0513). The evident peaks in the XRD of the electrode are at the 2 θ positions of 17°, 23.3°, 31.2°, 37°, and 43° which correspond to the lattice parameters of (200), (220), (400), (420), and (422) related to the CuHCF, respectively. Furthermore, the peaks at the 2 θ positions of 26°, 41°, 44°, 50°, 54°, 59°, and 70° are attributed to the graphite substrate. Figure 1 displays that the CuHCF is successfully deposited on the graphite current collector.

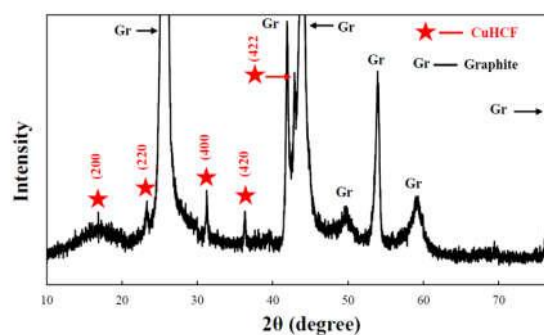


Figure 1. XRD pattern of the as-prepared CuHCF electrode.

The composition of the as-prepared CuHCF electrode was further determined by EDS elemental analysis. The EDS spectrum is illustrated in Fig. 2. Based on the intensity of the EDS spectrum, the relative stoichiometric ratio of K, Cu, and Fe elements is estimated to be 0.13:1.43:1 after normalizing regarding Fe content.

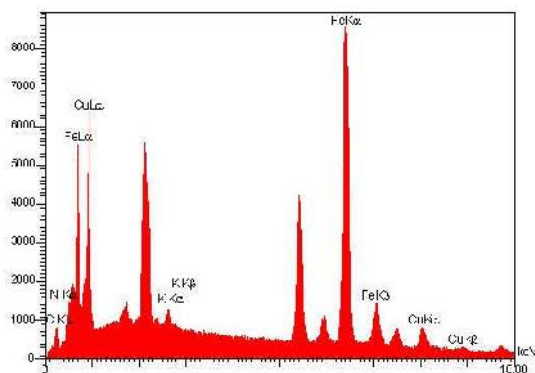


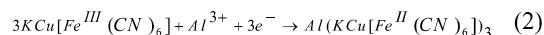
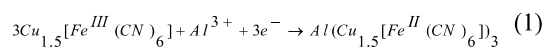
Figure 2. EDS spectrum of the as-prepared CuHCF film

In order to investigate the morphology of the CuHCF electrode, the FESEM images of the as-prepared electrode are shown in Fig. 3. The CuHCF nanoparticles with a semi-spherical morphology are uniformly distributed on the graphite substrate, as indicated in Fig. 3. The average particle size of the CuHCF active material is around 60 nm. Generally, the fine particles can facilitate electrolyte ions diffusion which result in improving the specific capacitance and rate performance. Moreover, the high specific surface area is expected to be obtained for the electrode material because of its fine particle size which leads to a facile electron and aluminum ion transfer in the electrode structure through fast kinetics and low polarization.

3.2. ELECTROCHEMICAL PERFORMANCE

To evaluate the electrochemical performance of the CuHCF in Al^{3+} ion-containing aqueous solution, the three-electrode cell is fabricated and then the CV and GCD tests were conducted. Figure 4 shows the CV curves of the CuHCF electrode in 0.5 M $Al_2(SO_4)_3$ aqueous solution at the scan rates of 5 and 10 $mV s^{-1}$. As can be seen, two anodic and cathodic peaks were observed for each curve, which can be assigned to the two-step aluminum ion intercalation/de-intercalation reaction into the CuHCF [19]. The peaks in the cathodic direction are related to the aluminum ion intercalation into the CuHCF electrode material concurrent with the charge storage. Additionally, the peaks in the anodic sweep direction are related to the aluminum ion extraction from the CuHCF concurrent with the charge release [20,21]. Two pairs of redox peaks can correspond to the reversible insertion/extraction of Al^{3+} into/from

potassium-free and potassium-containing CuHCF nanoparticles, respectively, as follows [22,23]:



In addition, by increasing the scan rate, the CV curves shapes remain unchanged and the position of the oxidation and reduction peaks slightly shifts to the higher and lower potentials, respectively. It suggests a relatively low internal resistance of the binder-free CuHCF electrode which may be due to the good contact between the graphite current collector and CuHCF active material.

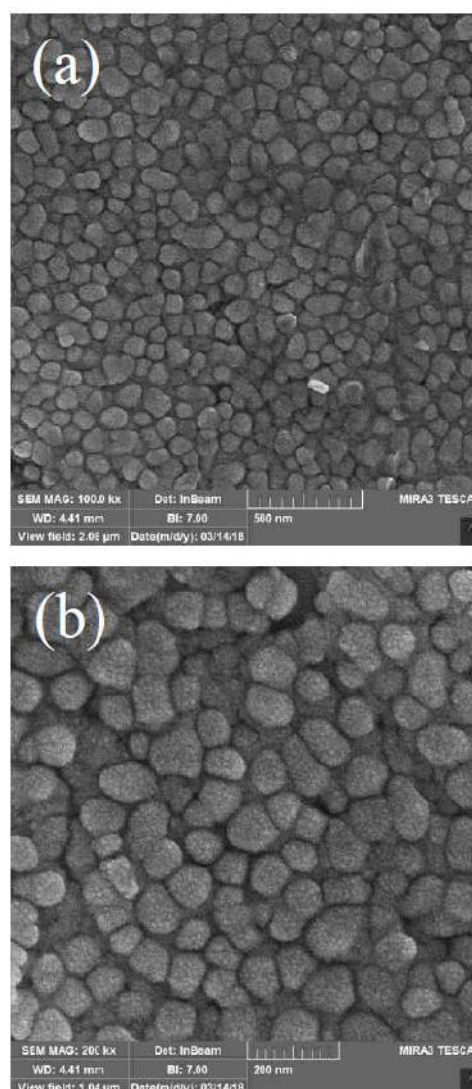


Figure 3. FESEM images of the CuHCF nanoparticles electrodeposited on graphite substrate

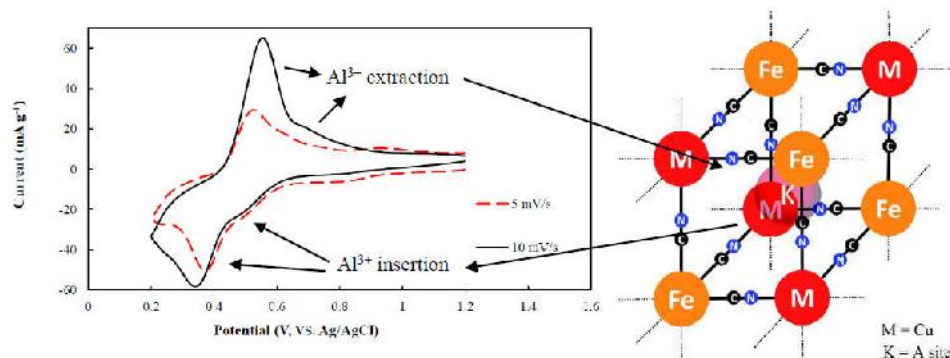


Figure 4. CV curves of the CuHCF electrode in the aqueous Al₂(SO₄)₃ and schematic positions of Al³⁺ in the CuHCF framework

To further evaluate the Al³⁺ storage in the prepared CuHCF electrode, the GCD measurements were conducted at various current densities, as depicted in Fig. 5. Two sloping voltage plateaus are observed in the discharge process which correspond to the two cathodic peaks in the CV curve.

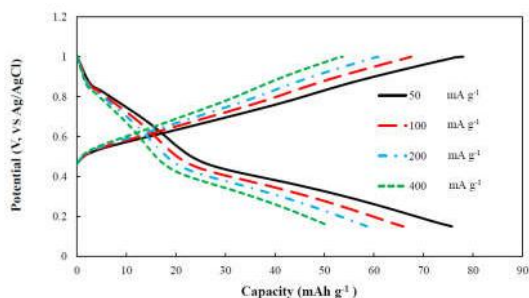


Figure 5. Galvanostatic charge-discharge curves of the CuHCF electrode at various current densities in the 0.5 M Al₂(SO₄)₃ aqueous solution

The calculated specific capacities of the CuHCF electrode versus current density are shown in Fig. 6. As can be seen, the as-prepared cathode exhibits the discharge capacities of 75.75, 65.90, 58.53 and 50.80 mAh g⁻¹ at the discharge rates of 50, 100, 200 and 400 mA g⁻¹, respectively, which are higher than those reported in previous literature [18]. It means that the as-prepared cathode presents a discharge capacity loss of 67.1% when the current rate increases from 50 to 400 mA g⁻¹ (equal to 8 times fold). The continuous drops in the specific capacitance of the electrode decreases via increasing the discharge current density which is because of the poor charge transfer process and slow diffusion of the electrolyte ions into all the inner microstructures of the electrode material [24]. This condition causes a less complete redox reaction of the active material, hence, the capacitance loss by increasing the discharge current rate. However, the improved capacities and rate performance of the prepared binder-free CuHCF compared to the

previous conventional ones [18] can be attributed to the higher electronic conductivity in the absence of insulating PVDF binder which provides fast and efficient transport of the electron and electrolyte ion for the electrochemical utilization of the active material.

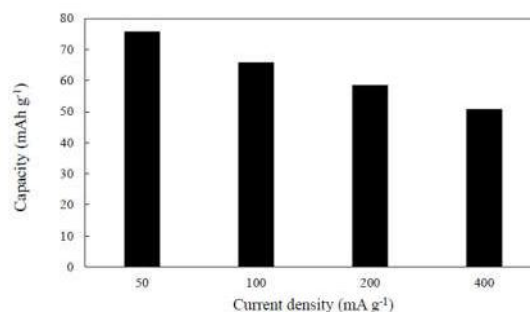


Figure 6. Specific capacities of the CuHCF electrode as the cathode of the aqueous-based Al-ion battery at various discharge current densities

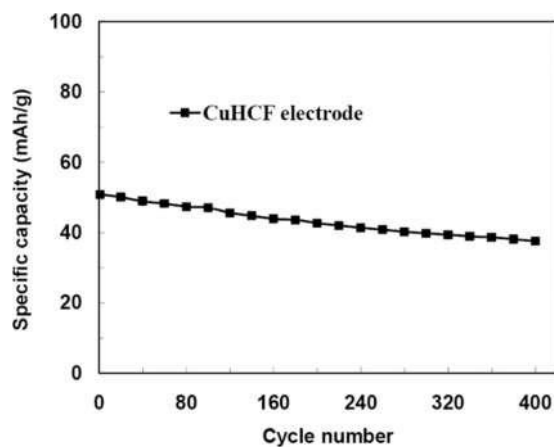


Figure 7. Cycle stability of the CuHCF electrode at a current density of 400 mA g⁻¹

Cycle life stability at the high current density is a key factor for practical application of the electrode material. Hence, we investigated the cycle life performance of the CuHCF electrode over 100 cycles at a high current density of 400 mA g⁻¹. As can be seen in Fig. 7, after 400 charge-discharge cycles, the specific capacitance of the CuHCF electrode decreases from 50.8 mAh g⁻¹ to 37.8 mAh g⁻¹ (degraded by 25.6%) suggesting its reasonable cycling stability in the aqueous electrolyte.

4. CONCLUSION

In summary, the binder-free CuHCF electrode was successfully prepared by a simple, fast and scalable pulse galvanostatic electrodeposition method on a graphite substrate without any polymeric binder. Formation of FCC nanostructure of Prussian blue was confirmed by XRD analysis. The as-prepared CuHCF electrode exhibited the ability of inserting the aluminum ion into the aqueous solution reversibly, making it a potential cathode for the aqueous Al ion batteries. The prepared electrode presented the highest Al storage performance with the best specific capacitances of 75.7 and 50.8 mAh g⁻¹ at 50 and 400 mA g⁻¹, respectively, and reasonable cycling stability (74.4% retention rate after 400 cycles) compared to the previously reported CuHCF electrode.

5. ACKNOWLEDGMENTS

The authors would like to express their gratitude to Iran National Science Foundation (INSF) for its support (Grant Number: 96010146).

6. REFERENCES

1. Yang, Z., Zhang, J., Kintner-Meyer, M. C., Lu X., Choi D., Lemmon J. P. and Liu J., Yang, Z., Zhang, J., Kintner-Meyer, M. C., Lu X., Choi D., Lemmon J. P. and Liu J., "Electrochemical energy storage for green grid", *chemical reviews*, Vol. 111, No. 5, (2011), 3577-3613.
2. Kalantarian M. M., Asgari S., "Theoretical Assessment of the First Cycle Transition, Structural Stability and Electrochemical Properties of Li₂FeSiO₄ as a Cathode Material for Li-ion Battery", *Advanced Ceramics Progress*, Vol. 3, No. 4, (2017), 25-33.
3. Kalantarian M. M., Oghbaei M., Asgari S., Karimi L., Ferrari S., Capsoni D., Bini M., Mustarelli P., "Electrochemical Characterization of Low-Cost Lithium-Iron Orthosilicate Samples as Cathode Materials of Lithium-Ion Battery", *Advanced Ceramics Progress*, Vol. 3, No. 3, (2017), 19-25.
4. Slater, M. D., Kim, D., Lee, E. and Johnson, C. S., "Sodium-Ion Batteries", *Advanced Functional Materials*, Vol. 23, No. 8, (2013), 947-958.
5. Qian, J. F., Zhou, M., Cao, Y. L., Ai, X. P. and Yang, H. X., "Nanosized Na₄Fe(CN)₆/C Composite as a Low-Cost and High-Rate Cathode Material for Sodium-Ion Batteries", *Advanced Functional Materials*, Vol. 2, No. 4, (2012), 410-414.
6. Su, D. W., Dou, S. X. and Wang, G. X., "Hierarchical orthorhombic V₂O₅ hollow nanospheres as high performance cathode materials for sodium-ion batteries", *Journal of Materials Chemistry A*, Vol. 2, No. 29, (2014), 11185-11194.
7. Fang, Y., Xiao, L., Qian, J., Ai, X., Yang, H., and Cao, Y., "Mesoporous Amorphous FePO₄ Nanospheres as High-Performance Cathode Material for Sodium-Ion Batteries", *Nano letters*, Vol. 14, No 6, (2014), 3539-3543.
8. Wang, W., Jiang, B., Xiong, W., Sun, H., Lin, Z., Hu, L., Tu, J., Hou, J., Zhu, H. and Jiao, S., "A new cathode material for super-valent battery based on aluminium ion intercalation and deintercalation", *Scientific Reports*, Vol. 3, No. 1, (2013), 3383-3388.
9. Levi, E., Gershinshy, G., Aurbach, D., Isnard, O. and Ceder, G., "New Insight on the Unusually High Ionic Mobility in Chevrel Phases", *Chemistry of Materials*, Vol. 21, No. 7, (2009), 1390-1399.
10. Jayaprakash, N., Das, S. and Archer, L., "The rechargeable aluminum-ion battery", *Chemical Communications*, Vol. 47, No. 47, (2011), 12610-12612.
11. Kazazi, M., Abdollahi, P. and Mirzaei-Moghadam, M., "High surface area TiO₂ nanospheres as a high-rate anode material for aqueous aluminium-ion batteries", *Solid State Ionics*, Vol. 300, No. 2, (2017), 32-37.
12. Kazazi, M., Zafar, Z.A., Delshad, M., Cervenka, J. and Chen, C., "TiO₂/CNT nanocomposite as an improved anode material for aqueous rechargeable aluminum batteries", *Solid State Ionics*, Vol. 3, No. 1, (2018), 64-69.
13. Neff, V. D., "Electrochemical Oxidation and Reduction of Thin Films of Prussian Blue", *Journal of The Electrochemical Society*, Vol. 125, No. 6, (1978), 886-887.
14. Itaya, K., Uchida, I. and Neff, V. D., "Electrochemistry of polynuclear transition metal cyanides: Prussian blue and its analogues", *Accounts of Chemical Research*, Vol. 19, No. 6, (1986), 162-168.
15. Stilwell, D. E., Park, K. H. and Miles, M. H., "Electrochemical studies of the factors influencing the cycle stability of Prussian Blue films", *Journal of Applied Electrochemistry*, Vol. 22, No. 4, (1992), 325-331.
16. de Tacconi, N. R., Rajeshwar, K. and Lezna, R. O., "Metal Hexacyanoferrates: Electrosynthesis, in Situ Characterization, and Applications", *Chemistry of Materials*, Vol. 15, No. 16, (2003), 3046-3062.
17. Rosi, N. L., Eckert, J., Eddaoudi, M., Vodak, D. T., Kim, J., O'Keeffe, M. and Yaghi, O. M., "Hydrogen Storage in Microporous Metal-Organic Frameworks", *Science*, Vol. 300, No. 5622, (2003), 1127-1129.
18. Liu, S., Pan, G. L., Li, G. R. and Gao, X. P., "Copper hexacyanoferrate nanoparticles as cathode material for aqueous Al-ion batteries", *Journal of Materials Chemistry A*, Vol. 3, No. 3, (2015), 959-962.
19. Wang, R. Y., Wessells, C. D., Huggins, R. A. and Cui, Y., "Highly Reversible Open Framework Nanoscale Electrodes for Divalent Ion Batteries", *Nano Letters*, Vol. 13, No. 11, (2013), 5748-5752.
20. Wessells, C. D., Peddada, C. V., McDowell, M. T., Huggins, R. A. and Cui, Y., "The Effect of Insertion Species on Nanostructured Open Framework Hexacyanoferrate Battery Electrodes", *Journal of The Electrochemical Society*, Vol. 159, No. 2, (2012), A98-A103.
21. Jia, Z., Wang, J. and Wang, Y., "Electrochemical sodium storage of copper hexacyanoferrate with a well-defined open framework for sodium ion batteries", *RSC Advances*, Vol. 4, No. 43, (2014), 22768-22774.
22. Mazeikiene R., Niaura G., Malinauskas A., "Electrochemical redox processes at cobalt hexacyanoferrate modified electrodes: An in situ Raman spectroelectrochemical study", *Journal of Electroanalytical Chemistry*, Vol. 719, No. 1, (2014), 60-71.
23. Yang Y., Hao Y., yuan J., Niu L., Xia F., "In situ co-deposition of nickel hexacyanoferrate nanocubes on the reduced graphene oxides for supercapacitors", *Carbon*, Vol. 84, No. 1, (2015) 174-184.
24. Kazazi M., "Facile preparation of nanoflake-structured nickel oxide/carbon nanotube composite films by electrophoretic deposition as binder-free electrodes for high-performance pseudocapacitors", *Current Applied Physics*, Vol. 17, No. 2, (2017), 240-248.